Available online at www.sciencedirect.com
ScienceDirect
Journal of Molecular Catalysis A: Chemical 267 (2007) 272–279
JOURNAL OF MOLECULAR CATALYSIS A: CHEMICAL
www.elsevier.com/locate/molcata

In-containing BEA zeolite for selective catalytic reduction of NO_x Part II. Relation between In active sites and catalytic activity

Oscar A. Anunziata [a,*], Andrea R. Beltramone [a], Eduardo J. Lede [b], Felix G. Requejo [b]

[a] *Grupo Fisicoquímica de Nuevos Materiales/Centro de Investigación y Tecnología Química (CITeQ), Universidad Tecnológica Nacional, Facultad Regional Córdoba, Maestro Lopez esq. Cruz Roja s/n, 5016 Córdoba, Argentina*
[b] *Instituto de Investigaciones Fisicoquímicas Teóricas y Aplicadas (INIFTA) e Instituto de Física La Plata (IFLP), Fac. de Cs. Exactas. Universidad Nacional de La Plata, Argentina*

Received 4 October 2006; accepted 28 November 2006
Available online 8 December 2006

Abstract

In-containing BEA zeolites showed high activity and selectivity for the nitrogen oxides selective catalytic reduction with methane in presence of oxygen. Perturbed angular correlation (PAC) characterization combined with Fourier transformed infrared spectroscopy (FTIR) of intermediates adspecies and reaction experiments, allowed us to correlate the catalytic activity with the nature of the active sites of the catalysts. The catalyst activity was affected by strong Brönsted sites and the type of In precursor and was influenced by the indium loading methods. Indium species were incorporated into the matrix using two different methods: ion exchange in liquid phase and ion exchange in solid phase, the first one presented a better performance in the SCR reaction.
© 2006 Elsevier B.V. All rights reserved.

Keywords: In-BEA; PAC; FTIR of adsorbed species; NO_x-SCR

1. Introduction

In Part I of this work, we showed the effect of preparation method of BEA-zeolite and the indium loading method on the performance for NO_x-SCR with methane in presence of oxygen. Temperature programmed ammonium desorption, XRD, BET, NMR-MAS of ^{27}Al and Fourier transformed infrared spectroscopy (FTIR) of pyridine adsorbed on the samples, allowed us to correlate the catalytic activity with the nature of the active sites of the catalysts. The catalyst activity was affected by strong Bronsted sites and the type of In precursor ($InCl_3$ and In_2O_3) and was influenced by the indium loading methods. The ion exchange in liquid phase method resulted in a higher activity than ion exchange in solid phase method. The BEA zeolite was obtained by means of a new and fast process of synthesis. This method reduces the aluminum as octahedral one (EFAL), diminishes the period of crystallization to 48–60 h, increases the percentage of crystallinity of the material and diminishes the content of the template agent, reducing the costs. The incorporation of indium did not modify the zeolite framework stability. The incorporation of In by ion exchange in liquid phase diminished the presence of ammonium cation as counter ion. The concentration of strong Brönsted acid sites decreased whereas the strong Lewis acid sites increased. Pyridine retained for the zeolite at different temperature followed by FTIR indicated that new and strong Lewis acid sites in In-HBEA zeolites are formed in concordance with TPD analysis.

Here we report a new series of PAC experiments performed on In/H-BEA catalysts prepared by different methods (synthesis reported in Part I) using ^{111}In as a probe.

The perturbed angular correlation (PAC) technique is a useful characterization tool for catalytic systems as it allows *in situ* studies of dispersed and diluted (as low as ppm) phases on catalysts [1–8]. This technique, by measurement of the local electric field gradient (EFG) at the radioactive probe site, can provide information on the characteristics (coordination, symmetry, distortions, etc.) of the different environments of the radioactive probes, their concentrations, and modifications related to *in situ*

* Corresponding author. Tel.: +54 351 4690585; fax: +54 351 4690585.
E-mail address: oanunziata@scdt.frc.utn.edu.ar (O.A. Anunziata).

1381-1169/$ – see front matter © 2006 Elsevier B.V. All rights reserved.
doi:10.1016/j.molcata.2006.11.056

conditions. This is possible because of the hyperfine interaction between the nucleus of the probe and the EFG produced by the extranuclear (ion and electronic) charges [3]. A brief and clear description of this technique and of the typical equipment setup was published by Vogdt et al. [9]. PAC gives direct information on site structure. Moreover, PAC experiments are a powerful aid to quantify the concentrations of molybdenum species identified by these techniques. Compounds containing molybdenum have the advantage that after neutron irradiation the PAC probe 99Mo is formed from natural 98Mo present in the samples. Thus, the extracted information is reliable since the PAC probe does not introduce an impurity. In the case of In-supported catalysts, the time differential observations of the perturbed angular correlation of γ-rays emitted from radioactive ^{111}In (probe) allowed the characterization of different In sites (and In species). Since the EFG depends on r^{-3} (where r is the distance between the probe and the charge), PAC characterizations are very sensitive to distances, the PAC technique becoming a local environment characterization technique. Thus, PAC experiments are very appropriate for characterizing species with different local environments and/or short range order (as in the case of species exchanged in zeolites).

Wodniecki et al. [10] studied nickel–indium intermetallic compounds of different stoichiometries by means of the perturbed angular correlation spectroscopy. They measured the temperature dependence of the hyperfine interaction parameters for ^{111}Cd probes in the crystal lattices of Ni_3 In_7 and Ni_2 In_3 and found a T character of the electric field gradient temperature dependence.

It has been suggested that the activity of the In-ZSM5 catalyst for the SCR reaction is due to the presence of $(InO)^+$ groups [11]. We have previously reported the first PAC characterization of this species [12]. We supported the fact that the activation of methane is initiated by NO_2 and NO_3^- chemisorbed species on InO^+ sites of the In-ZSM-5 zeolite [13].

In Part I we showed the effect of BEA zeolite topology [14], and the incorporation of active In species by IELP (ion exchange liquid phase) and IESP (ion exchange in solid phase) on the catalytic activity.

In this work, PAC characterization combined with FTIR of $NO/CH_4/O_2$ co-adsorption experiments and the earlier results of XRD, TPAD and the reaction experiments reported in Part I, will help us to elucidate the nature of the In species present in the catalysts, and the intermediate NO_x adspecies responsible of the selective reduction of NO_x with methane in the presence of excess oxygen.

2. Experimental

2.1. Catalysts preparation

The preparation methods of the catalysts were reported in Part I of this work. A summary of the different samples used in this study are listed below:

- Sample A: In-HBEA prepared by ion exchange in liquid phase, Si/Al molar ratio: 23, In content: 2% w/w.
- Sample AM: "as made", In_2O_3-HBEA prepared by ionic exchange in solid phase, Si/Al molar ratio: 23, In content: 2% w/w.
- Sample B: AM Sample reduced under H_2 flow of 5 ml/min and 2 °C/min from 100 °C to 500 °C, holding this temperature during 12 h, then it is oxidized at 500 °C under oxygen flow of 10 ml/min and 2 °C/min from 100 °C and calcined during 12 h at 500 °C.
- Sample C: AM Sample reduced under H_2 atmosphere from 100 to 300 °C and then oxidized at 500 °C.

2.2. Catalytic activity

The studies on the catalytic activity were carried out using a flow reactor of simple step, made of silica fused with an internal diameter of 5 mm and 300 mm in length, loaded with 0.5 g of catalyst, at atmospheric pressure. The reactant mixture was obtained from independent gases lines and controlled by controller of mass flow, to obtain 1000 ppm of NO, 1000 ppm of CH_4 and 10% of O_2, using He as carrier gas. The resulting GHSV was set to 30,000 h^{-1} based on the bed density of 0.5 g/cm^3 for zeolites. The range of temperatures used was between 300 and 600 °C. The reaction products were analyzed by gas chromatography, using a column of silica–alumina/Porapak Q of 2 m in length and a TC-Mass detector.

2.3. Catalysts characterization

2.3.1. Studies by Fourier transformed infrared spectroscopy

Infrared analysis of H-BEA and In-HBEA were performed on a JASCO 5300 spectrometer using a thermostatized cell with CaF_2 windows connected to a vacuum line, with a self-supported wafer adsorbed at 10^{-3} Torr and desorbed at 350–400 °C at 10^{-3} Torr for 4 h. $NO/CH_4/O_2$ co-adsorption experiments with In-HBEA samples were carried out using a thermostatized cell with CaF_2 windows connected to a vacuum line, with a self-supported wafer.

For NO adsorption, the samples were purged in vacuum for 6 h before NO was introduced into the cell. All spectra were recorded at room temperature as a function of exposure time. For the quantitative comparison of absorbance, we took the absolute value of absorbance per milligram of sample at different wave numbers. These values were obtained from the FTIR spectra. A reference spectrum of the sample before exposure of NO was subtracted from each spectrum.

2.4. Perturbed angular correlation technique

The time differential observation of the perturbed angular correlation of γ-rays emitted from radioactive ^{111}In allows us to characterize different In species by means of hyperfine interactions. The principle of the application of PAC to In can be found elsewhere [15]. This technique by means of the determination of the gradient of local electric field in the site of a probe atom, can give information on the characteristics (coordination, symmetry, distortion, etc.) of the different surroundings from the probe, its concentrations and modifications by in-situ analysis conditions

(temperature, atmosphere, pressure, etc.). Often, a probe of PAC is introduced as an impurity but in this case, the information of the PAC turns out to be more reliable since the probe does not constitute an impurity but that it is a natural component of the catalyst.

3. Results and discussion

3.1. Studies by Fourier transformed infrared spectroscopy

FTIR data of acid sites as a function of pyridine retained at 350 and above 400 °C are shown in Table 1 (data reported in Part I).

3.2. Adsorption of nitrogen monoxide

The introduction of NO (250 Torr, equilibrium pressure for 30 min, followed by a 15 min evacuation) to the calcined In-HBEA samples and subsequent evacuation (10^{-1} Torr) is shown in Fig. 1 When NO was introduced to the samples, two strong peaks were observed from FTIR spectrum of Samples A, B and C at room temperature, the bands at 1665 cm^{-1} is likely due to adsorbed NO_3^- [16–18] and the band at 1620 cm^{-1} is assigned to NO_2 adsorbed over InO^+ site [13,19] (see Fig. 1 A–C). This suggests that NO molecules are weakly adsorbed and some of them were oxidized to NO_2 and nitrate species by the residual O_2 species weakly adsorbed on the catalyst. The results of the adsorption of NO (250 Torr) at 400 °C on In-HBEA samples are showed in Fig. 1 A_1–C_1. We can observe, at this temperature, that only the 1620 cm^{-1} band remains in all the samples.

The comparison between the intensities of the peaks for the different species adsorbed in the three samples at room temperature is illustrated in the Fig. 2a. The band at 1620 cm^{-1} has higher intensity in Sample A than B or C. This specie is one of the most important intermediates in the CH4-SCR process. The 1665 cm^{-1} band is more intense in Samples A and C. Fig. 2b shows the intensities of the peaks in the three samples at 400 °C. At this adsorption temperature the intensity of the bands diminished sharply, but NO_2 specie remains adsorbed over the samples in an appreciable amount. This fact indicates that NO_2 species adsorbed over In-sites are the intermediates for the reduction of NO to N_2.

Table 1
FTIR data of acid sites as a function of pyridine retained at 350 °C and above 400 °C, respectively on H-BEA and In-HBEA

Catalysts	Brönsted sites[a]		Lewis sites[a]	
temperature [°C] desorption of pyridine	350	400	350	400
H-BEA	0.180	0.150	0.040	0.020
Sample A	0.032	0.014	0.170	0.140
Sample B	0.065	0.030	0.120	0.090
Sample C	0.100	0.080	0.090	0.070
Sample AM	0.180	0.150	0.040	0.020

[a] FTIR, pyridine mmol/g retained at different temperatures before desorption at 10^{-4} Torr for 4 h.

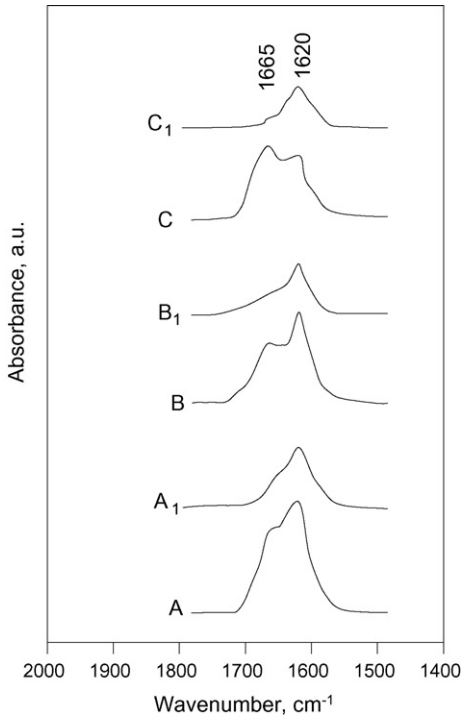

Fig. 1. FTIR spectra of NO adsorbed (250 Torr equilibrium pressure, after of vacuum activation at 500 °C) on In-HBEA, Samples A, B and C, (A, B, C: NO adsorbed at 25 °C; A_1, B_1 and C_1: NO adsorbed at 400 °C).

3.3. Co-adsorption of nitrogen monoxide, methane and oxygen at 400 °C

The results of the co-adsorption of NO, CH_4 and O_2 (250 Torr of NO, 250 Torr of CH_4, 250 Torr of O_2 equilibrium pressure for 30 min, followed by a 15 min evacuation) at 400 °C on In-HBEA samples are shown in Fig. 3. According to our experimental results, the NO_2 and NO_3^- adspecies showed an increase when oxygen and methane was introduced with NO. Oxygen improved NO adsorption, clearly due to oxida-

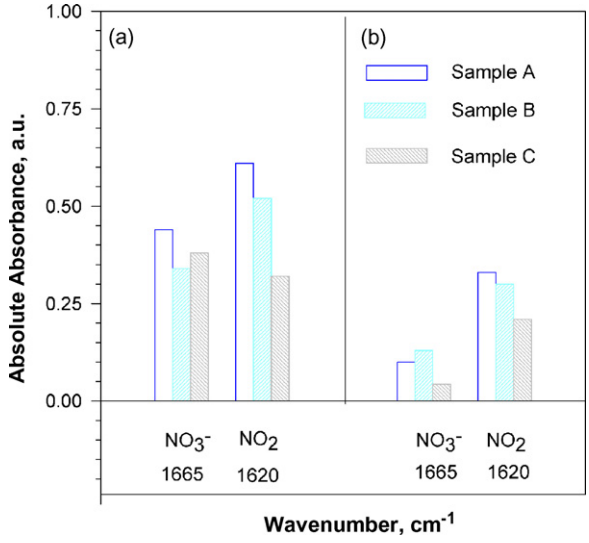

Fig. 2. Adsorption of NO over In-HBEA, Samples A, B and C, (a) NO adsorbed at 25 °C; (b) NO adsorbed at 400 °C.

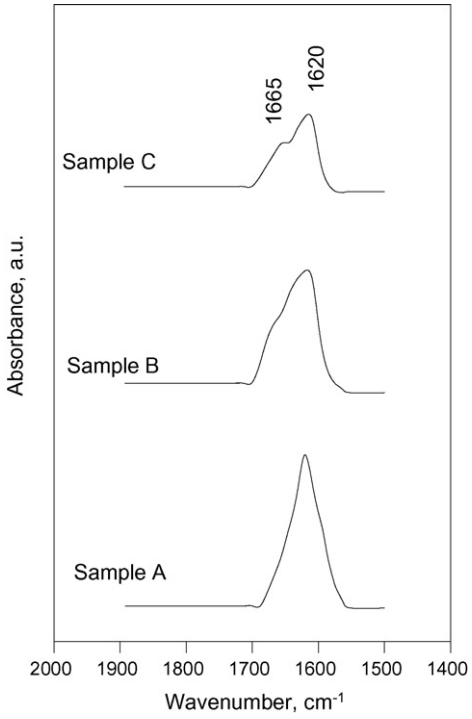

Fig. 3. FTIR spectra of $NO + CH_4 + O_2$ (NO: 250 Torr; CH_4: 250 Torr, O_2: 250 Torr) co-adsorbed on In-HBEA at 400 °C, Samples A, B and C.

tion of NO to NO_2 and nitrate species. The NO_y adspecies, with high intensities, were observed on the NO_2 adsorbed over several zeolites [20–22], suggesting stronger adsorption for NO_2 than NO.

Comparing the data of absorbance from the spectra obtained at 400 °C, we observe that the Sample A possesses more intermediate species adsorbed (NO_2–In-site) than the others samples, particularly than the Sample C (see Fig. 4).

The bands assigned to these adspecies are present even, at the catalytic reaction temperature, indicating that NO_2 and NO_3^- adspecies might play an important role in the SCR of NO_x over

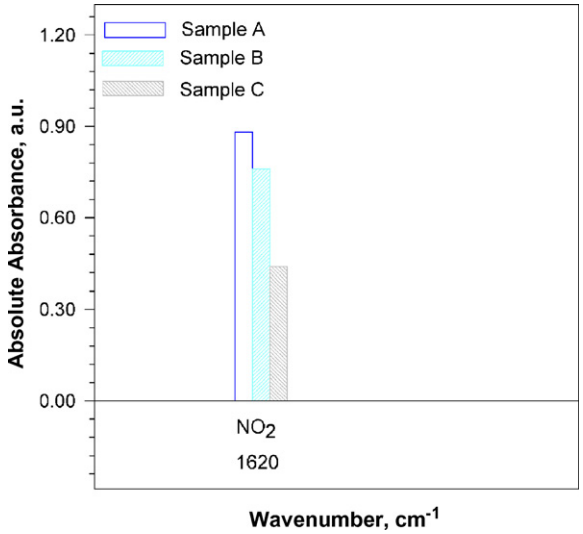

Fig. 4. Co-adsorption of $NO + CH_4 + O_2$ over In-HBEA at 400 °C, Samples A, B and C.

Table 2
Catalytic activity of In-HBEA at different temperatures for NO-SCR

Sample	NO conversion to N_2 (mol%)			Methane conversion (mol%)		
	A	B	C	A	B	C
Temperature (°C)						
400	60	60	59	33	49	69
450	80.5	79	72	55	80	94
500	78	78	77	77.5	99	100
550	76	76	64.8	99	99.1	100

NO conversion to N_2, and methane conversion for Sample A: IELP activated in air at 500 °C; Sample B: IESP reduced at 500 °C under H_2 and then oxidized at 500 °C; Sample C: IESP reduced under H_2 at 300 °C and then oxidized in air a 500 °C.

In-containing zeolite, in agreement with our recent work [13] and Ogura et al. [11].

3.4. Catalytic activity

The results of the catalytic activity for the selective reduction of NO with methane in the presence of oxygen are summarized in Table 2. As we can see, the conversion of NO reached approximately an 80% for Samples A and B at 450 °C and the methane conversion was 55 and 80% for the Samples A and B, respectively.

With the objective to analyze the concerted action of active In-species and H^+ sites of the catalysts (Samples A, B and C), we chose the reaction temperature of 400 °C, taking in account that at this temperature we studied the adsorbed species from $NO/CH_4/O_2$ reaction system and pyridine determined by FTIR. At this temperature the NO conversion to N_2 was 60 mol% for all the samples, but the methane conversion was different for each

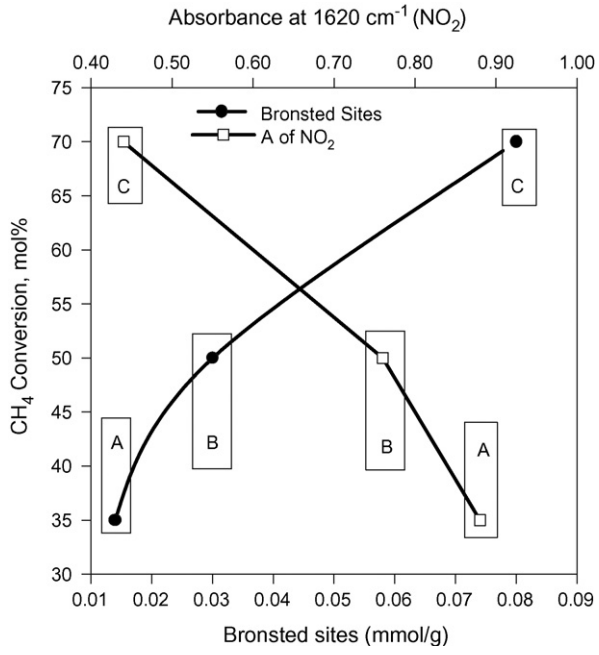

Fig. 5. Relationship between methane conversion at 400 °C and ($-NO_2$) adsorbed specie and Brönsted sites for Samples A, B and C.

samples. Therefore, in Fig. 5 we show only the methane conversion as a function of NO_2-adspecies absorbance and the Brönsted acid sites at 400 °C (according to the data of Figs. 3 and 4, and Table 1, respectively).

The graph shows that the methane conversion is indeed higher over the Sample C, accordingly with the highest value of Brönsted sites. For this sample, methane conversion increases with the reaction temperature (>400 °C), but the NO conversion is constant or decreases. Methane is converted to CO and CO_2 over H^+ sites, but it is not consumed to reduce NO at these temperatures. Sample A possesses more NO_2-adspecies and less Brönsted sites and these sites are capable to convert methane selectively to reduce NO to N_2. So, the selective methane conversion for the samples presents the following order: Sample A > B > C in concordance with NO_2-species and Lewis acids sites of the catalyst.

For Samples A and B the active sites are capable to form species with high thermal stability [23], therefore, chemisorbed NO_x begin to reduce it self to N_2 at lower temperature than on In-ZSM-5 zeolite [15]. In that case, the maximum NO conversion to N_2 using methane as reducer was 80 mol% at 540 °C. However, for In-HBEA, Samples A and B reach similar conversion levels but at lower temperature (450 °C). In the case of In-ZSM-5, the conversion was 30 mol% lower than for In-HBEA at this reaction temperature [15].

These differences seem to indicate that the amount and/or nature of the active sites in both zeolites are not quite similar, like will be able to be seen in the following section about PAC characterization.

3.5. PAC Characterization of In-HBEA zeolite

3.5.1. In-HBEA, IELP

Fig. 6 shows the spectra of precession of spin ($R(t)$) and its Fourier transform for Sample A. The values of the fitted hyperfine parameters are shown in Table 3. The fit was made proposing three hyperfine interactions and the obtained results indicate the presence of at least two In species. The sites associated with the assemblies of parameters 1 and 2 correspond with reported for In_2O_3 [15]. The parameter 3 correspond to a different In-site, more likely due to In exchanged by ammonium ions in zeolite framework. This specie was previously associated to InO^+ in In-ZSM-5 [15].

3.5.2. In-HBEA, IESP

The PAC spectrum showed in Fig. 7, correspond to the obtained $R(t)$ and its Fourier transform for In-HBEA. In Sample AM: as made, the spectrum shows the characteristic signal of the In_2O_3 that we used in its preparation and it does not show any interaction with the zeolite. The values of the fit hyperfine parameters (sites AM.1 and AM.2 in Table 3) confirm it.

Considering that the IESP of In_2O_3 over NH_4-BEA, was interpreted by Mihályi et al. [24] as the reduction of In_2O_3 to univalent indium concomitantly incorporated by solid-state

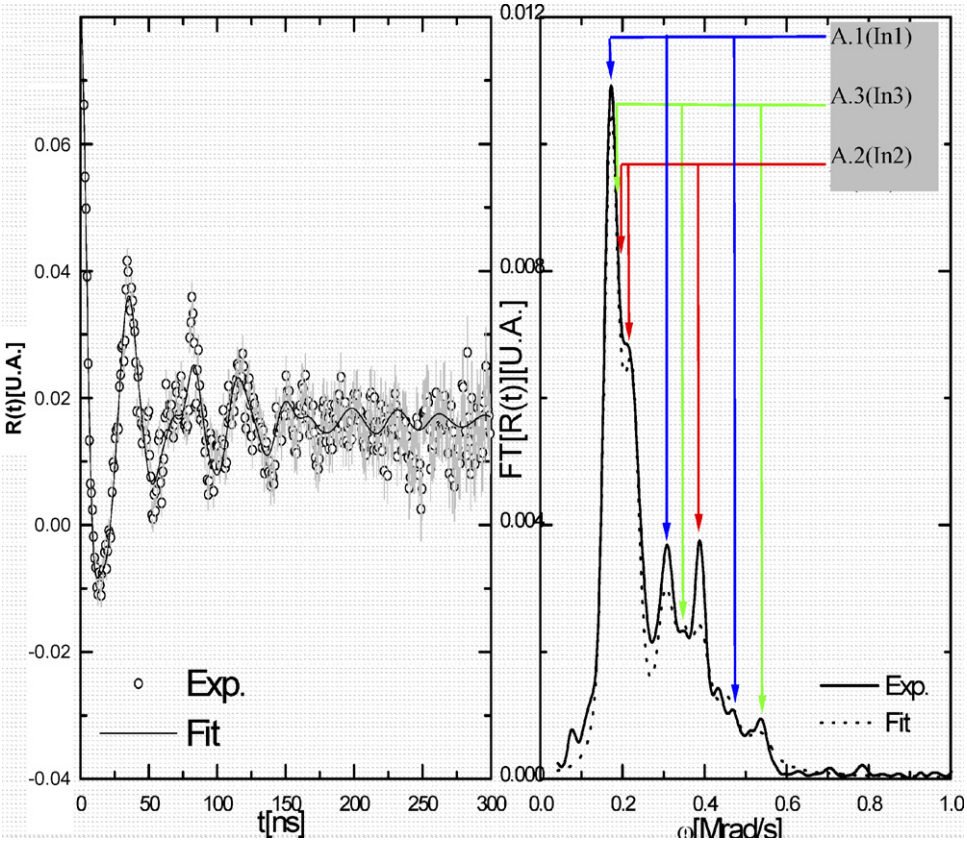

Fig. 6. PAC Spectra (left) and its Fourier transform (right) of Sample A, measured at 500 °C in air. The arrows indicate the three harmonic components for each hyperfine interaction.

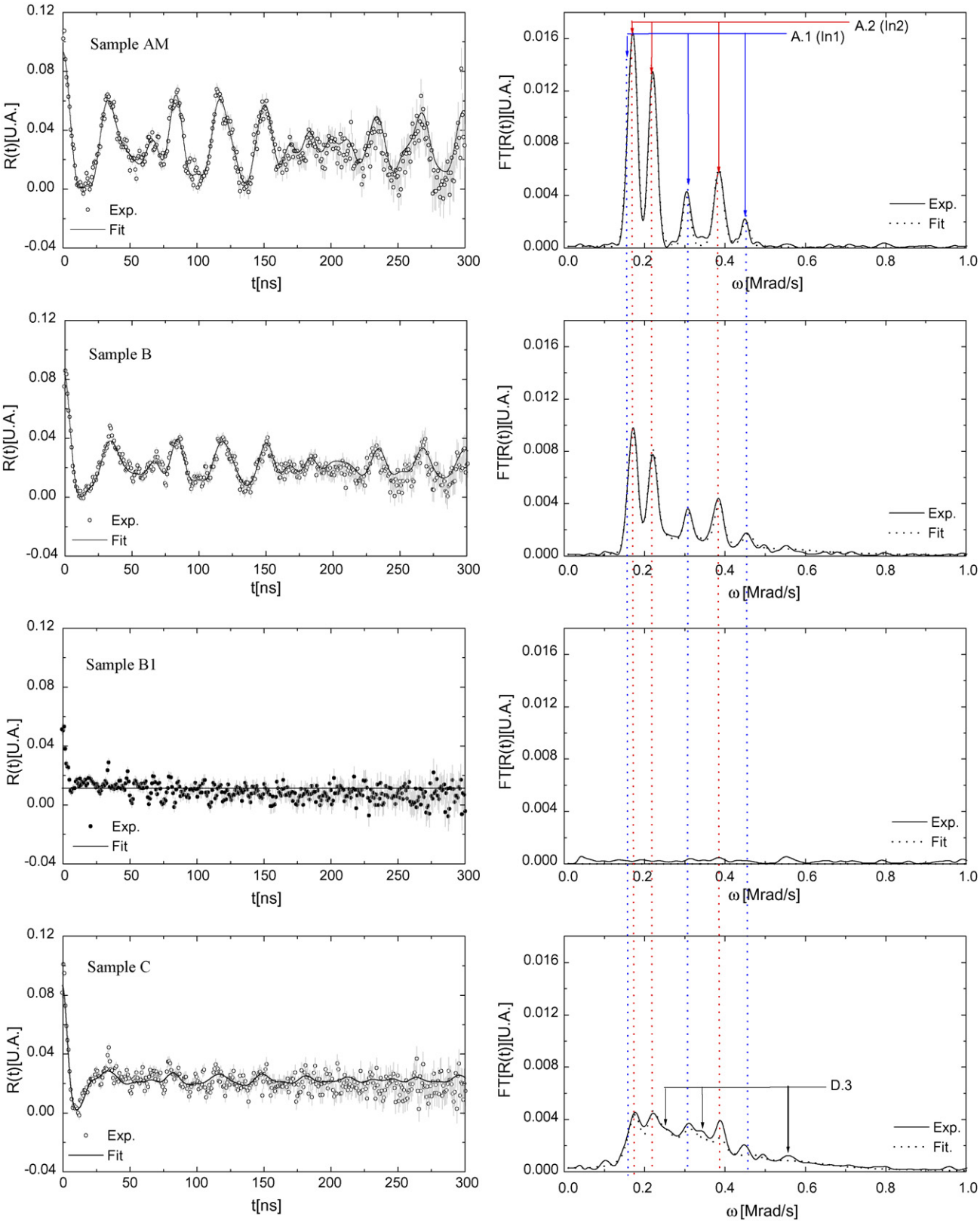

Fig. 7. PAC Spectra (left) and its Fourier transform (right) of In-HBEA by IESP: Sample AM; Sample B; Sample B1; Sample C.

Table 3
Values of the fitted hyperfine parameters in the spectra showed in Figs. 6 and 7

Catalyst	Site	Population f (%)	Frequency ω_Q (Mrad./s)	Asymmetry parameter (n)	Distribution δ (%)
Sample A	A.1	33 (12)	24.9 (2)	0.17 (3)	5.8 (9)
	A.2	57 (4)	19.3 (1)	0.71 (1)	5.8 (6)
	A.3	**10 (4)**	**28.7 (2)**	**0.33 (2)**	**2 (1)**
AM[a]	AM.1	20.1 (5)	24.72 (6)	0.02 (4)	0.2 (3)
	AM.2	80 (2)	19.09 (3)	0.699 (3)	1.2 (1)
Sample B	B.1	16 (3)	24.96 (9)	0.11 (3)	1.1 (6)
	B.2	36 (3)	19.10 (3)	0.705 (5)	0.7 (3)
	B.3	**48 (9)**	**29 (2)**	**0.42 (6)**	**21 (4)**
Sample C	C.1	16 (2)	25.5 (4)	0.18 (8)	5 (2)
	C.2	7 (1)	19.2 (1)	0.76 (2)	0 (2)
	C.3	**78 (16)**	**33.1 (9)**	**0.50 (5)**	**19 (3)**
In_2O_3[b]	In1	23 (2)	24.38 (8)	0	0.16 (6)
	In2	77 (2)	18.71 (8)	0.71 (1)	0.22 (6)

[a] AM: As made, ion exchange solid phase. Sample B without the oxidizing process (B1) can be fitted with a relaxation for all In-sites (f = 100%).
[b] Hyperfine parameters of bulk In_2O_3 measured at 600 °C [15].

ion to form $2In^+Z^-$ and the degree of oxidation by oxygen to InO^+-Z^- is a function of the temperature (450 °C to reduce and the oxidation process), we reduced at 300 and 500 °C and oxidized at 500 °C to observe the effect in the formation of InO^+ species (Sample B and C). The reductive pretreatment temperature of the catalysts (500 °C) for Sample B, was chosen to be below the dehydroxylation temperature of the zeolite but sufficiently high for complete reduction of In_2O_3. Sample B reduced in controlled atmosphere of H2 during 2 h at 500 °C and later oxidizing in air at 500 °C for 1 h, was analyzed by PAC and the $R(t)$ spectra and its Fourier transform are clearly different from the previous ones, admit an adjustment with three interactions. The presence of In on sites with similar surroundings to In in In_2O_3 is again observed. We found hyperfine parameters associated to a second specie of In interacting with the BEA zeolite (see Table 3, B.1, 2, 3 sites). To show the effect of the reduction of In-HBEA, we prepared other sample reduced at 500 °C but its PAC measurements was made without oxidizing it. The results are indicated as Sample B1 (see Fig. 7). In these conditions the PAC spectrum showed a remarkable change. The interpretation of this signal is not even conclusive but it could be due to stationary dynamic at the probe's surrounding, like chemisorption and desorption of H_2, which would take place in the order of few nseg. Similar results were previously reported through TDPAC experiments on In/H-ZSM5, In/FER and InPt/FER in presence of H_2 [25,26].

Sample C obtained by a processing of reduction in controlled atmosphere by constant flow of H_2 during 2 h at 300 °C and later oxidizing in air at 500 °C for 1 h, was measured by PAC at 500 °C in air. An appreciable change in comparison with *AM* is observed. This spectra was fit with three interactions, two of which (sites C.1 and C.2 in Table 3) are in agree with both sites of Indium in In_2O_3. The third interaction (site C.3 in Table 3) would correspond to second specie of In interacting with the zeolite framework, with high population but at higher frequency (ω_Q) and with higher asymmetry parameter than for the specie present in the Sample A. These values suggest that the indium species interacting with BEA zeolite (Sample C) seem to be quiet different to the indium species found in Sample A. In the same way, the high EFG (electric field gradient) distribution of B.3 and C.3 (21 and 19, respectively, see Table 3) would also explained by several anchoring configurations of the (InO^+) species because of the size of this species can be found within the channel of the zeolite. Thus, not all of B.3 and C.3 can be assigned to active InO^+ species [27]. However, a very low distribution of A.3 is found for Sample A (δ (%) = 2 in Table 3), indicating that, even at low concentration compared with the other samples, this signal is attributed to InO^+ active sites for SCR of NO, in concordance with the results of the catalytic activity and NO_2 intermediate adspecies showed in the FTIR analysis for Sample A.

4. Conclusions

A good correspondence between the catalytic activity and characterization of the materials was observed. The PAC technique allowed us to determine the presence of active sites such as InO^+ in Sample A (IELP) activated in air at 500 °C, showing hyperfine interactions (A.3 in Table 3) attributed to the presence of $(InO)^+$-BEA species and two In_2O_3 signals (hyperfine interactions A.1 and A.2). The samples prepared by IESP (B and C) reduced at 500 and 300 °C under H_2, respectively, and then oxidized at 500 °C, show two characteristic signals of In_2O_3 crystals. The third interaction (site B.3 and C.3 in Table 3) would correspond to a second specie of In interacting with the zeolite framework, with high population but at higher frequency (ω_Q) and with higher asymmetry parameter, thus not all of this signal (specially in Sample C) corresponds to InO^+ species as we found in Sample A.

FTIR of pyridine indicated that new and strong Lewis acid sites in In-HBEA zeolites are formed in concordance with TPD analysis. NO adsorption showed NO_3^- and NO_2 adspecies are the intermediate of the reaction.

The results obtained with In-HBEA prepared by IELP and IESP (reduced at 500 °C and then oxidized at 500 °C) are more active for the reduction of NO with methane than In-ZSM-5 [15]. In the same way, with these catalysts, methane is consumed selectively for the reduction of NO to N_2 at 450–500 °C,

especially for the sample obtained by ion exchange in liquid phase with $InCl_3$.

Acknowledgments

O.A.A., A.R.B. and F.G.R. CONICET researcher. O.A.A. and A.R.B. are grateful to CONICET Argentine, PIP 2005–2007, No. 6394 and. Foncyt PICT 2005–2008, No. 14–14485 and F.G.R. to CONICET and Fundación Antorchas of Argentina for financial support of their research.

References

[1] F.G. Requejo, A.G. Bibiloni, Phys. Status Solidi. A 148 (1995) 497.
[2] F.G. Requejo, A.G. Bibiloni, Langmuir 12 (1) (1996) 51.
[3] H. Frauenfelder, R.M. Steffen, in: K. Siegbahn (Ed.), Alpha-, Beta- and Gamma-Ray Spectroscopy, Vol. 2, Amsterdam, North-Holland, 1968, p. 997.
[4] G.L. Catchen, Mater. Res. Soc. Bull. 20 (1994) 37.
[5] G. Krausch, R. Fink, K. Jacobs, U. Kohl, J. Lohmuller, B. Luckscheiter, R. Platzer, B.-U. Runge, U. Wohrmann, G. Schatz, Hyperfine Interact. 78 (1993) 261.
[6] G. Krausch, T. Detzel, R. Fink, B. Luckscheiter, R. Platzer, U. Wohrmann, G. Schatz, Phys. Rev. Lett. 68 (1992) 377.
[7] J.M. Adams, J. Fu, G.L. Catchen, D.L. Miller, G.L. Catchen, Surf. Sci. 337 (1995) 118.
[8] J.M. Adams, Ph.D. Dissertation, The Pennsylvania State University, 1995.
[9] C. Vogdt, T. Butz, A. Lerf, H. Knözinger, J. Catal. 31 (1989) 116.
[10] P. Wodniecki, B. Wodniecka, M. Marszałek, A. Kulinska, A.Z. Hrynkiewicz, J. Alloys Compd. 267 (1998) 14–18.
[11] M. Ogura, M. Hayashi, E. Kikuchi, Catal. Today 42 (1998) 159.
[12] E. Miro, L. Gutierrez, J.M. Ramallo Lopez, F.G. Requejo, J. Catal. 188 (1999) 375–384.
[13] A. Beltramone, L. Pierella, F. Requejo, O. Anunziata, Catal. Lett. 91 (1–2) (2003) 19.
[14] O. Anunziata, L. Pierella, Stud. Surf. Scie. and Catal. 125 (1999) 481.
[15] F. Requejo, J. Ramallo-López, E. Lede, E. Miró, L. Pierella, O. Anunziata, Catal. Today 54 (1999) 553.
[16] K. Hadjiivanov, D. Klissurski, G. Ramis, G. Busca, Appl. Catal. B 7 (1996) 251.
[17] E. Ivanova, K. Hadjiivanov, D. Klissurski, M. Bevilacqua, T. Armaroli, G. Busca, Micro. Meso. Mater. 46 (2001) 299.
[18] M. Kantcheva, Appl. Catal. B 42 (2003) 89.
[19] E. Kikuchi, M. Ogura, Catal. Surveys Japan 1 (1997) 227.
[20] R. Long, R. Yang, J. Catal. 194 (2000) 80.
[21] H. Chen, E.M. El-Malki, X. Wang, R. van Santen, W. Sachtler, J. Mol. Catal. A 162 (2000) 159.
[22] L. Lobree, I. Hwang, J. Reimer, A. Bell, J. Catal. 186 (1999) 242.
[23] M. Mihaylov, K. Hadjiivanov, D. Panayotov, Appl. Catal. B 51 (1) (2004) 33.
[24] R.M. Mihályi, H.K. Beyer, V. Mavrodinova, Ch. Minchev, Y. Neinska, Micro. Meso. Mater. 24 (4–6) (1998) 143.
[25] J.M. Ramallo-Lopez, A.G. Bibiloni, F.G. Requejo, L.B. Gutierrez, E.E. Miro, J. Phys. Chem. B 106 (2002) 7815.
[26] V. Mavrodinova, M. Papova, M. Mihalyi, G. Pal-Borbely, Ch. Minchev, Appl. Catal. A 262 (2004) 75.
[27] J.M. Ramallo Lopez, M. Renteria, E. Miro, F. Requejo, A. Traverse, Phys. Review Lett. 91 (10) (2003) 108304–108311.